International Conference on Nuclear Data for Science and Technology 2007
DOI: 10.1051/ndata:07732

Measurement of the ^{90,91,92,93,94,96}Zr(n,γ) and ^{139}La(n,γ) cross sections at n_TOF

G. Tagliente[1,a], U. Abbondanno[2], G. Aerts[3], H. Álvarez[4], F. Álvarez-Velarde[5], S. Andriamonje[3], J. Andrzejewski[6], P. Assimakopoulos[†7], L. Audouin[8], G. Badurek[9], P. Baumann[10], F. Bečvář[11], E. Berthoumieux[3], F. Calviño[12], M. Calviani[13,14], D. Cano-Ott[5], R. Capote[15,16], C. Carrapiço[17,3], P. Cennini[18], V. Chepel[19], E. Chiaveri[18], N. Colonna[1], G. Cortes[20], A. Couture[21], J. Cox[21], M. Dahlfors[18], S. David[8], I. Dillmann[22], C. Domingo-Pardo[23,22], W. Dridi[3], I. Duran[4], C. Eleftheriadis[24], M. Embid-Segura[5], L. Ferrant[†8], A. Ferrari[18], R. Ferreira-Marques[19], K. Fujii[2], W. Furman[25], I. Goncalves[19], E. González-Romero[5], F. Gramegna[13], C. Guerrero[5], F. Gunsing[3], B. Haas[26], R. Haight[27], M. Heil[22], A. Herrera-Martinez[18], M. Igashira[28], E. Jericha[9], F. Käppeler[22], Y. Kadi[18], D. Karadimos[7], D. Karamanis[7], M. Kerveno[10], P. Koehler[29], E. Kossionides[30], M. Krtička[11], C. Lampoudis[24,3], H. Leeb[9], A. Lindote[19], I. Lopes[19], M. Lozano[16], S. Lukic[10], J. Marganiec[6], S. Marrone[1], T. Martínez[5], C. Massimi[31], P. Mastinu[13], A. Mengoni[15,18], P.M. Milazzo[2], C. Moreau[2], M. Mosconi[22], F. Neves[19], H. Oberhummer[9], S. O'Brien[21], J. Pancin[3], C. Papachristodoulou[7], C. Papadopoulos[32], C. Paradela[4], N. Patronis[7], A. Pavlik[33], P. Pavlopoulos[34], L. Perrot[3], M.T. Pigni[9], R. Plag[22], A. Plompen[35], A. Plukis[3], A. Poch[20], J. Praena[13], C. Pretel[20], J. Quesada[16], T. Rauscher[36], R. Reifarth[27], C. Rubbia[37], G. Rudolf[10], P. Rullhusen[35], J. Salgado[17], C. Santos[17], L. Sarchiapone[18], I. Savvidis[24], C. Stephan[8], J.L. Tain[23], L. Tassan-Got[8], L. Tavora[17], R. Terlizzi[1], G. Vannini[31], P. Vaz[17], A. Ventura[38], D. Villamarin[5], M.C. Vincente[5], V. Vlachoudis[18], R. Vlastou[32], F. Voss[22], S. Walter[22], M. Wiescher[21], and K. Wisshak[22]

The n_TOF Collaboration (www.cern.ch/ntof)

[1]Istituto Nazionale di Fisica Nucleare, Bari, Italy – [2]Istituto Nazionale di Fisica Nucleare, Trieste, Italy – [3]CEA/Saclay-DSM/DAPNIA, Gif-sur-Yvette, France – [4]Universidade de Santiago de Compostela, Spain – [5]Centro de Investigaciones Energeticas Medioambientales y Tecnologicas, Madrid, Spain – [6]University of Lodz, Lodz, Poland – [7]University of Ioannina, Greece – [8]Centre National de la Recherche Scientifique/IN2P3-IPN, Orsay, France – [9]Atominstitut der Österreichischen Universitäten, Technische Universität Wien, Austria – [10]Centre National de la Recherche Scientifique/IN2P3-IReS, Strasbourg, France – [11]Charles University, Prague, Czech Republic – [12]Universidad Politecnica de Madrid, Spain – [13]Istituto Nazionale di Fisica Nucleare, Laboratori Nazionali di Legnaro, Italy – [14]Dipartimento di Fisica, Università di Padova, Italy – [15]International Atomic Energy Agency (IAEA), Nuclear Data Section, Vienna, Austria – [16]Universidad de Sevilla, Spain – [17]Instituto Tecnológico e Nuclear (ITN), Lisbon, Portugal – [18]CERN, Geneva, Switzerland – [19]LIP-Coimbra & Departamento de Fisica da Universidade de Coimbra, Portugal – [20]Universitat Politecnica de Catalunya, Barcelona, Spain – [21]University of Notre Dame, Notre Dame, USA – [22]Forschungszentrum Karlsruhe GmbH (FZK), Institut für Kernphysik, Germany – [23]Instituto de Física Corpuscular, CSIC-Universidad de Valencia, Spain – [24]Aristotle University of Thessaloniki, Greece – [25]Joint Institute for Nuclear Research, Frank Laboratory of Neutron Physics, Dubna, Russia – [26]Centre National de la Recherche Scientifique/IN2P3-CENBG, Bordeaux, France – [27]Los Alamos National Laboratory, New Mexico, USA – [28]Tokyo Institute of Technology, Tokyo, Japan – [29]Oak Ridge National Laboratory, Physics Division, Oak Ridge, USA – [30]NCSR, Athens, Greece – [31]Dipartimento di Fisica, Università di Bologna, and Sezione INFN di Bologna, Italy – [32]National Technical University of Athens, Greece – [33]Institut für Isotopenforschung und Kernphysik, Universität Wien, Austria – [34]Pôle Universitaire Léonard de Vinci, Paris-La Défense, France – [35]CEC-JRC-IRMM, Geel, Belgium – [36]Department of Physics - University of Basel, Switzerland – [37]Università degli Studi Pavia, Pavia, Italy – [38]ENEA, Bologna, Italy

Abstract. Neutron capture cross sections of Zr and La isotopes have important implications in the field of nuclear astrophysics as well as in the nuclear technology. In particular the Zr isotopes play a key role for the determination of the neutron density in the He burning zone of the Red Giant star, while the ^{139}La is important to monitor the s-process abundances from Ba up to Pb. Zr is also largely used as structural materials of traditional and advanced nuclear reactors. The nuclear resonance parameters and the cross section of ^{90,91,92,93,94,96}Zr and ^{139}La have been measured at the n_TOF facility at CERN. Based on these data the capture resonance strength and the Maxwellian-averaged cross section were calculated.

1 Introduction

The neutron capture cross sections of ^{90,91,92,93,94,96}Zr and ^{139}La has been measured with high resolution at the n_TOF facility at CERN.

The neutron capture measurement of these isotopes has a particular relevance in the nuclear astrophysics, since the Zr belongs to the first s-process peak in the solar abundance distribution at N = 50 while the La belongs to the second s-process peak at N = 82. The ^{90}Zr and the ^{139}La are neutron magic and are characterized, like the ^{91,92,93,94}Zr, by a low neutron capture cross section and are predominately of s-process origin. The most neutron reach Zr stable isotope, ^{96}Zr, is traditionally considered to be an r-only isotope with a small s-process admixture refs. [1,2]. Its abundance is considered to be a strong indicator in the efficiency of the ^{22}Ne neutron source during the He shell burning episodes of thermally pulsing AGB stars.

The lanthanum acts as bottleneck between the abundant light n-capture element of the first s-process peak and the

[a] Presenting author, e-mail: giuseppe.tagliente@ba.infn.it

heavy elements from Sm up to Pb and Bi, it is very important for interpreting the element abundance patterns in very old, metal poor stars. Since the La abundance is completely represented by ^{139}La it can be used to distinguish the s-process components from the products of explosive r-process nucleosynthesis, the s/r ratio is of utmost importance for the galatical chemical evolution. The major motivation of the present measurement was to reduce the uncertainties to a few percent, as required to improve the stellar s-process model.

2 Experimental set-up

The measurements were performed at the neutron time-of-flight (n_TOF) facility at CERN in a range of energy between 1 eV and 1 MeV with a pulsed neutron beam. The neutrons were generated by spallation reactions induced by a pulse of beam of 20 GeV protons impinging on a massive lead target. The low repetition rate of the proton beam driver, the extremely high instantaneous neutron flux, the low background conditions in the experimental area, together with improved neutron sensitivity of the γ-ray detectors make this facility unique for neutron induced reaction cross section measurements with high accuracy. The main characteristics of the facility and apparatus are reported in [3].

2.1 Detectors and data acquisition

The measurement is based on the detection of the γ rays emitted in the de-excitation cascade following a neutron capture event. Two C_6D_6 detectors with minimized neutron sensitivity [4], placed perpendicular to the neutron beam at a distance of about 3 cm from the beam axis, were used to detect the γ rays. The background due to in-beam γ rays was reduced by placing the detectors 9.2 cm upstream of the sample position. The light output of the detectors was calibrated by means of the ^{137}Cs,^{60}Co and Pu/C γ-ray sources. The calibrated neutron time of flight was used to determine the neutron energy. Measured upstream of the capture samples with low mass flux monitor consisting of a Mylar foil 1.5 μm in thickness with a layer of 200 μg/cm^2 of ^{6}Li surrounded by four silicon detectors outside the neutron beam, measuring the charged particles of the ^{6}Li(n,α)^{3}H reaction [14]. The data were acquired with high frequency flash ADC (FADC) using the standard n_TOF data acquisition system [5]. The raw data were recorded signal by signal for a detailed off-line analysis, which allows one to extract the required information on timing, charge, amplitude and particle identification, allowing in particular an efficient γ-n discrimination.

2.2 Samples

The characteristic of the samples are summarized in table 1. The enriched Zr samples were prepared from oxide powder, an admixture of Hf, Na, Mg, Al, Sn and Mo were also present in the Zr samples. The influence of those contaminants, although small (their total contamination was lower than 1%), can not be neglected. Additional Au reference sample as well as a natural C and ^{208}Pb sample were used for neutron flux normalization in the measurements. The Au reference sample was used because the gold capture cross section is known with high accuracy, particularly the saturated resonance at 4.9 eV. The C and ^{208}Pb samples were used to determine the background components related to sample scattered neutrons and in-beam γ rays.

Table 1. Samples characteristics. The Zr samples where in the ZrO_2 form.

Sample	Diam. (mm)	Mass (g)	Enrich. (%)
^{90}Zr	22	2.721	97.7
^{91}Zr	22	1.407	89.9
^{92}Zr	22	1.351	91.4
^{93}Zr	22	6.595	91.4
^{94}Zr	22	2.015	19.98
^{96}Zr	22	3.401	58.5
^{139}Zr	20	1.934	99.71

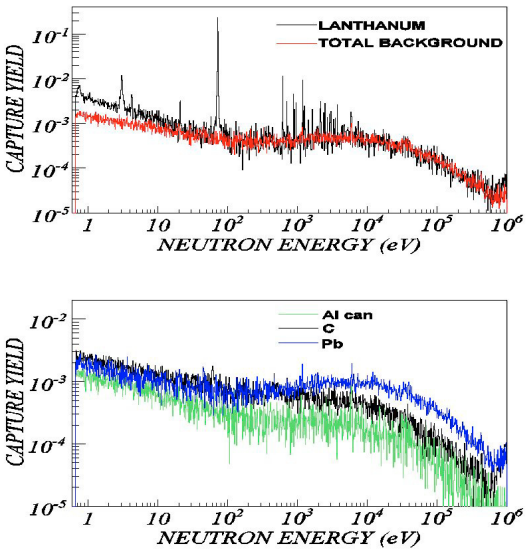

Fig. 1. Capture yield of the La sample and total background. Bottom: Individual background components [8].

3 Data analysis

The main steps of the data analysis are: an accurate calibration of the C_6D_6 detectors, ambient and sample related backgrounds determination and subtraction by means of the spectra measured with an empty Al can, and with a Pb and C sample, the absolute normalization of the capture yields made with an accuracy of 3% via the spectrum measured with a Au sample. The efficiency correction was performed with the Pulse Height Weighting Technique (PHWT) [6] applied to the C_6D_6 capture data in order to achieve a cascade detection independent of the particular de-excitation path. The respective weighting functions are sensitive to the experimental set-up, including the investigated sample. These functions were derived by detailed Monte Carlo simulations. Figure 1 shows the capture yield for the ^{139}La sample compared to the total background and the individual background components.

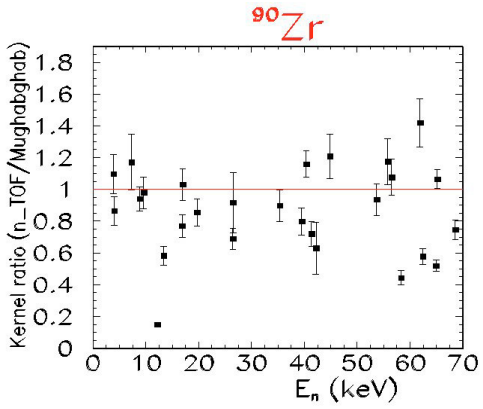

Fig. 2. Ratio of the ^{90}Zr capture kernels measured in n_TOF with data from Mughabghab compilation.

Finally, systematic uncertainties are significantly reduced by the improved n_TOF set-up, which exhibits much lower neutron sensitivity by the use of low-mass carbon fibre cans for the liquid scintillator detectors. In addition, the use of FADCs provides an efficient way for n/γ-discrimination.

4 Results

Resonances observed were analyzed in terms of R-matrix parameters in the Reich-Moore approximation with the code SAMMY [8]. Due to the high energy resolution of the n_TOF facility many new resonances were found. The resonance parameters measured at n_TOF are for all the Zr samples in general 10–20% smaller than previously reported while for the La sample are 10% lower than that reported in [9] and a few percent lower than that reported in [10]. A possible explanation for these systematic differences can be due to a more reliable evaluation of the PHWT, an accurate treatment of the corrections for self shielding, multiple scattering and the effect of neutron energy resolution, and the use of the well tested R-matrix code SAMMY. Figure 2 shows the comparison of the neutron capture kernels $g\Gamma_\gamma\Gamma_n/\Gamma_{\rm tot}$ for the ^{90}Zr resonances with those reported in the Mughabghab compilation [11].

4.1 Maxwellian averaged capture cross section

In order to study the s-process abundances, the Maxwellian averaged cross sections (MACS) are required over a range of thermal energies. The MACS were calculated folding the capture cross section with a maxwellian distribution of the neutron fluence in a wide energy range (1 eV–550 keV).

Since the n_TOF data cover part of this spectrum, only the partial contribution to MACS can be accurately determined. To calculate the MACS in the full energy range the JENDL cross section were renormalized with respect to the n_TOF data.

Figure 3 shows the comparison between the MACS calculated for the ^{96}Zr with n_TOF data and the JENDL 3.3 library and figure 4 shows the comparison of MACS calculated for the ^{139}La with n_TOF data and the one calculated from an FZK with activation method [15] and

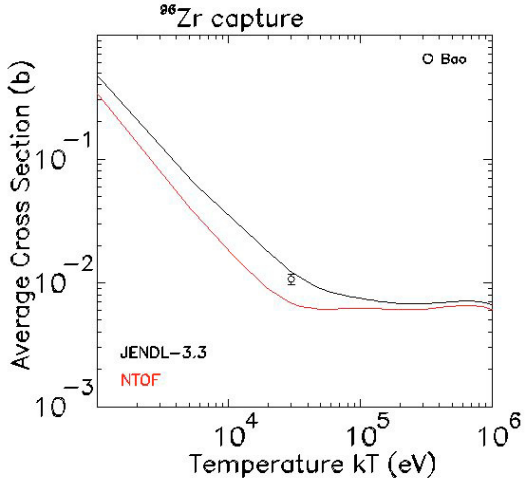

Fig. 3. Comparison between the ^{96}Zr MACS calculated with n_TOF data and the JENDL3.3 data.

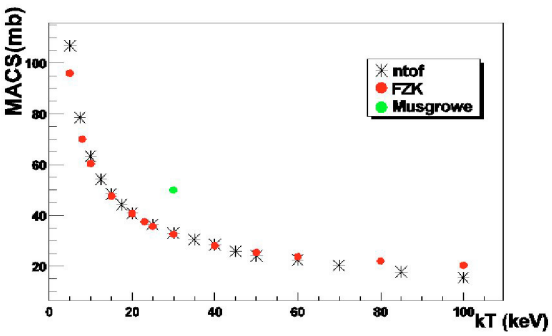

Fig. 4. Comparison among the ^{139}La MACS calculated with n_TOF data and FZK and Musgrowe data.

Table 2. MACS calculated wit n_TOF data compared with recommended values of the previous data.

Isotope	n_TOF	Bao et al. [13]
^{90}Zr	18.1 ± 1	21 ± 2
^{91}Zr	51.6 ± 2	60 ± 8
^{92}Zr	29.7 ± 2	33 ± 4
^{94}Zr	27.6 ± 1	26 ± 1
^{96}Zr	7.5 ± 0.4	10.7 ± 0.5
^{139}Zr	32.4 ± 3	38.4 ± 2.7

Musgrowe data. In table 2 the values calculated for the MACSs are compared with recommended values derived from previous data [13]. The MACS calculated on the present experimental data except for the ^{94}Zr result lower than those reported in literature, although apart for the ^{96}Zr the new values are within the error bars of the previous data.

5 Conclusions

The (n,γ) cross sections of the ^{90,91,92,93,94,96}Zr and ^{139}La have been measured over a wide neutron energy range using the innovative features of the n_TOF CERN facility. The capture kernel presented in this work are for all sample except for ^{94}Zr weaker than what reported in the previous measurements and

in the libraries evaluated data. This result can be explained in terms of the optimized performance of the facility, experimental set-up, data acquisition and the more accurate data analysis tools, as the PHWT and SAMMY code. The new capture cross section have led to an improvement of the MACS which were calculated with more accuracy and the values found results lower than the values recommended from the literature. Furthermore some other nuclear quantities has been calculated as the level density, which implication for the ^{139}La are published in [8].

This work was supported by the EC under contract FIKW-CT-2000-00107 and by funding agencies of the participating institutes.

References

1. F. Käppeler, Prog. Nucl. Part. Phys. **43**, 419 (1999).
2. K.A. Toukan, K. Debus, F. Käppeler, G. Reffo, Phys. Rev. C **51**, 1540 (1995).
3. C. Borcea et al., Nucl. Instrum. Meth. A **513**, 523 (2003).
4. R. Plag et al., Nucl. Instrum. Meth. A **496**, 425 (2003).
5. U. Abbondanno et al., Nucl. Instrum. Meth. A **538**, 692 (2005).
6. U. Abbondanno et al., Nucl. Instrum. Meth. A **521**, 454 (2004).
7. R. Terlizzi et al., Phys. Rev. C **75**, 35807 (2007).
8. N.M. Larson, Report ORNL/TM-979, Oak Ridge National Laboratory, 2000.
9. Y. Nakajima, N. Ohnishi, Y. Kanda, M. Mizumoto, Y. Kawarasaki, Y. Furuta, A. Asami, J. Nucl. Sci. Technol. **20**, 183 (1983).
10. L. Musgrove, B.J. Allen, R.L. Macklin, Australian J. Phys. **30**, 599 (1977).
11. S.F. Mughabghab, M. Divadeenam, N.E. Holden, *Neutron Cross Sections, Vol. 1, and Neutron Resonance Parameters and Thermal Cross Sections, Part A, Z = 1-60* (Academic Press, Orlando, 1981).
12. Z.Y. Bao et al., At. Data Nucl. Data Tables **76**, 70 (2000).
13. S. Marrone et al., Nucl. Instrum. Meth. A **513**, 692 (2003).
14. S. OBrien, S. Dababneh, M. Heil, F. Kppeler, R. Gallino, M. Pignatari, Astrophys. J. **647**, 685 (2006).
15. J.M. Smith, Eur. Phys. J. Appl. Phys. **25**, 123 (2004).